Optimizing the Earth–LISA ‘rendezvous’

2012 Class. Quantum Grav. 29 035009

(http://iopscience.iop.org/0264-9381/29/3/035009)

IOP PUBLISHING CLASSICAL AND QUANTUM GRAVITY

Class. Quantum Grav. **29** (2012) 035009 (16pp) doi:10.1088/0264-9381/29/3/035009

Optimizing the Earth–LISA 'rendezvous'

Fabrizio De Marchi[1,3,4], **Giuseppe Pucacco**[2] **and Massimo Bassan**[2]

[1] Department of Physics, Università di Trento and INFN, Sezione di Trento, I-38100 Povo, Italy
[2] Dipartimento di Fisica, Università di Roma 'Tor Vergata' and INFN, Sezione di Roma Tor Vergata, I-00133 Roma, Italy

E-mail: fdemarchi@roma2.infn.it

Received 14 July 2011, in final form 13 December 2011
Published 17 January 2012
Online at stacks.iop.org/CQG/29/035009

Abstract
We present a general survey of heliocentric LISA orbits, hoping that it might help in the exercise of rescoping the mission. We try to semi-analytically optimize the orbital parameters in order to minimize the disturbances coming from the Earth–LISA interaction. In a set of numerical simulations, we include non-autonomous perturbations and provide an estimate of Doppler shift and breathing as a function of the trailing angle.

PACS numbers: 04.80.nn, 95.10.Eg

(Some figures may appear in colour only in the online journal)

1. Introduction

The LISA space experiment to detect low-frequency gravitational waves has been for a long time a priority mission of space agencies, both in Europe and in the US. Recently, there has been ample discussion [1] on a possible scaled-down version of the LISA mission that, in order to meet tighter budget constraints, could be characterized by a shorter arm length ℓ, a closer mean distance from the Earth (a smaller trailing angle) and maybe a 2-arm (4-link) configuration, giving up the third arm. In this case, it becomes natural to consider a right angle geometry as an alternative to the traditional, 60°, equilateral triangle (ET). A discussion on a so-called New Gravitational Observatory (NGO) is underway within the LISA scientific community, and its state of the art is summarized in a continuously updated, unpublished document that goes under the name of *NGO Yellow Book* [2].

Although other configurations have been considered [1], these triangular 'constellations' on heliocentric Earth-trailing orbits still remain the favorite choice. We focus our attention on the evaluation of the usual kinematic indicators of performance (arm flexing, breathing angles and Doppler shifts) when reducing both the size of the triangle and the Earth–LISA/NGO

[3] Present address: Dipartimento di Fisica, Università di Roma 'Tor Vergata' and INFN, Sezione di Roma Tor Vergata, I-00133 Roma, Italy.
[4] Author to whom any correspondence should be addressed.

distance over the entire mission lifetime. As is well known, the interaction of LISA/NGO with the Earth is the major perturbation. The dominant effect is a parabolic drift characterized by a 'rendezvous' (RV) at which the distance between the constellation and the Earth is minimum. We investigate how additional perturbing effects influence the motion of LISA/NGO around the RV and how it is possible to optimize it.

In agreement with the science requirements summarized in the NGO Yellow Book we assume the following guidelines.

- Arm length: $\ell = 1$ Gm. This choice allows a substantial budget reduction while maintaining a useful bandwidth that extends down to below 3×10^{-3} Hz, preserving sensitivity to some important classes of astrophysical sources like, e.g., compact binaries. We consider two configurations: the ET with side ℓ and an isosceles right triangle (IRT) with two equal arms of length ℓ and the third one $\ell\sqrt{2}$ long. Although it might appear fair to compare configurations with the same sensitivity rather than same arm length (the sensitivity scales with the sine of the angle between the arms, and is therefore 14% better in an IRT), the ET has the added advantage of a third arm that increases its sensitivity, e.g., to stochastic signals[5].
- *Flexing.* The spacecraft (S/C) relative velocity in the sensitive axis (rate of change of the arm length) causes a Doppler shift of the laser frequency. Technical constraints on the laser phase meter [3] set a maximum bandwidth of 20 MHz over a $\lambda = 1.064$ μm carrier wavelength, corresponding to $V/c < 6.5 \times 10^{-8}$ or $V < 20$ m s^{-1}. For the sake of plot readability, we note that, as $\Delta f = V/\lambda$, the Doppler shift (in MHz) and the longitudinal velocity (in m s^{-1}) have approximately (within $\sim$6%) the same numerical value. This is the reason why our plots report Doppler shifts expressed in m s^{-1}.
- *Breathing angle.* The relative motion of S/Cs also imposes a continuous adjustment of the angle between two beams departing from the same corner, in order to track the opposite S/Cs; this fluctuation over the nominal angle (60° or 90°) is referred to as the breathing angle (BA). The telescope must therefore be continuously aligned by an optical assembly tracking mechanism, to keep this mechanism simple (and lightweight) its range should not exceed BA $< \pm 1.5°$.
- *Trailing angle (TA, also referred to as lag angle):* LISA/NGO follows the Earth on a heliocentric circular orbit and TA is the angle between the constellation and the Earth as seen from the Sun. TA is a good indicator of the Earth–LISA/NGO distance, because the radial secular motion (away from the Sun) of the constellation is normally much smaller than the tangential (along the Earth orbit) one. The Earth is the main perturbation source for the constellation, and a large distance would reduce its effects; however, communication constraints demand TA as small as possible, compatibly with the above requirements. Initial conditions are chosen in such a way that over the mission lifetime, TA will not exceed 21°.
- *Mission lifetime.* Six years[6].

The plan of the paper is as follows: we start by recalling the simple models describing the interaction between the Sun and LISA (section 2) and the Sun, Earth and LISA (section 3). In section 4, we describe an optimization method with the aim of an important reduction of

[5] An ET, having a smaller distance h from the constellation center (see equation (4)), is in principle more robust against orbit perturbations, although this does not show in our calculations. ET and IRT (both with $\ell = 1$ Gm) are the two configurations presently considered by the NGO Science Team for the mission reformulation: we conform to this choice.

[6] The 'New LISA' or 'NGO' mission is presently (December 2011) considered for a two years lifetime. This is, however, a recent result that has emerged during the refereeing process. At the time of writing the manuscript, an optimistic, high-end hypothesis of six years mission life was considered (Jennrich, private communication). It will be anyway always desirable, if conditions allow, to extend the duration as much as possible.

flexing, breathing angles and Doppler shifts. We test this method first on the simplified Sun–Earth–LISA/NGO model and then on a more complete model including the real gravitational effects due to the dynamics of the solar system. Finally, in section 5 conclusions are drawn.

While graphs and details are given below, we anticipate here some results.

- As far as Doppler and breathing requirements are concerned, a short LISA (an NGO) can safely be put in an orbit much closer to the Earth: TA $\approx 12^\circ$ at RV (the baseline design was 20°) or 31 Gm.
- Should we give up the third arm (keep only 4 optical links), a right-angled triangle can be employed and performs at least as well as the usual ET in several of the tests (Doppler, breathing, etc) we carried out.

2. Keplerian orbits

We describe the interaction of LISA/NGO with the Earth in the framework of the Hill–Clohessy–Wiltshire (HCW) system [4, 5]: this is a rotating reference frame where the equations of motion are calculated via standard Lagrangian methods. In this and the following section, we will assume the Sun at rest in an inertial reference frame. The origin of the HCW frame rotates around the Sun on a circular reference orbit of radius R_0 and with orthogonal axes oriented as follows: x is directed radially opposite to the Sun, y is in the direction tangent to the motion and z is perpendicular to the ecliptic. The time evolution of these orbits can be described with adequate precision using the post-epicyclic approximation in the HCW frame [6, 7].

2.1. Zeroth-order approximation

Under the effect of the Sun only, at zeroth order, the equations of motion for a S/C in the rotating frame are

$$\begin{aligned} &\ddot{x} - 2\omega\dot{y} - 3\omega^2 x = 0,\\ &\ddot{y} + 2\omega\dot{x} = 0,\\ &\ddot{z} + \omega^2 z = 0, \end{aligned} \tag{1}$$

where $\omega = \sqrt{GM_\odot/R_0^3}$ is the mean motion and the most general solution is a combination of an ellipse in the xy plane and an oscillation in the z direction

$$\begin{aligned} x(t) &= 2\left(2x_0 + \frac{\dot{y}_0}{\omega}\right) - \left(2\frac{\dot{y}_0}{\omega} + 3x_0\right)\cos\omega t + \frac{\dot{x}_0}{\omega}\sin\omega t,\\ y(t) &= y_0 - 2\,\frac{\dot{x}_0}{\omega} - 3\,(\dot{y}_0 + 2\omega x_0)\,t\, + 2\frac{\dot{x}_0}{\omega}\cos\omega t + 2\left(2\frac{\dot{y}_0}{\omega} + 3x_0\right)\sin\omega t,\\ z(t) &= z_0\cos\omega t + \frac{\dot{z}_0}{\omega}\sin\omega t. \end{aligned} \tag{2}$$

The first, most natural choice, that removes drifts and offsets, is to set $\dot{y}_0 = -2\omega x_0$ and $\dot{x}_0 = \omega y_0/2$, so that the trajectory is reduced to a combination of simple oscillations along the three axes. We shall later see, in section 4.2, how a different, more convenient initial condition can be chosen. Moreover, for a rigid, polygonal constellation, the distance of the S/C from the origin must be constant, say h, so that we obtain [8]

$$\dot{z}_0 = \pm\frac{\sqrt{3}}{2}\omega y_0, \quad z_0 = \pm\sqrt{3}x_0, \quad y_0 = \pm\sqrt{h^2 - 4x_0^2}, \quad x_0 = \pm\frac{h}{2}. \tag{3}$$

The orbit of one of the S/Cs in the HCW frame is a circular motion with constant angular velocity ω and radius h around the origin in a plane inclined at $\pm 60^\circ$ with respect to the xy

(ecliptic) plane. A second S/C, describing the same path (with a certain delay), will be at a constant distance ℓ, from the first one. For n such S/Cs, on the vertices of a regular polygon, their distance h from the origin and the relative phase delay are

$$h = \frac{\ell}{2\sin(\pi/n)}, \quad \phi = \frac{2\pi}{n}.$$

Finally, we choose $x_0 = +h/2$ to be consistent with the notations of [9, 6] and the zeroth-order orbits turn out to be

$$\mathbf{r}_k^{(0)}(t) = \frac{\ell}{2\sin(\pi/n)}\left[\frac{1}{2}\cos\sigma_k, \sin\sigma_k, \frac{\sqrt{3}}{2}\cos\sigma_k\right], \quad \sigma_k = \frac{2\pi(k-1)}{n} - \omega t. \tag{4}$$

The ET constellation is obtained with $n = 3$ and $k = 1, 2, 3$, while the IRT one corresponds to $n = 4$ (and $k = 1, 2, 3$), namely

$$\mathbf{r}_k^{(0)}(t) = \frac{\ell}{\sqrt{2}}\left[\frac{1}{2}\cos\sigma_k, \sin\sigma_k, \frac{\sqrt{3}}{2}\cos\sigma_k\right], \quad \sigma_k = (k-1)\frac{\pi}{2} - \omega t.$$

2.2. First-order approximation

The first optimization is possible by changing the tilt angle of the constellation, i.e. the inclination of the triangle with respect to the ecliptic. Introducing a parameter δ_1 [6] such that,

$$\pm 60^\circ + \delta_1 \frac{\ell}{2R_0},$$

the first-order corrections

$$\mathbf{r}_k^{(1)}(t) = \left(x_k^{(1)}, y_k^{(1)}, z_k^{(1)}\right), \tag{5}$$

are

$$\begin{aligned}
x_k^{(1)}(t) &= \frac{h^2}{2R_0}\left[\frac{3}{2}\left(\frac{1}{2} - \delta_1\right)\cos\sigma_k - \frac{1}{8}\cos 2\sigma_k - \frac{5}{8}\right],\\
y_k^{(1)}(t) &= \frac{h^2}{2R_0}\left[\left(\frac{3}{2} - 3\delta_1\right)\sin\sigma_k - \frac{1}{2}\sin 2\sigma_k\right],\\
z_k^{(1)}(t) &= \frac{h^2}{2R_0}\left[\frac{\sqrt{3}}{2}(\delta_1 - 1)\cos\sigma_k - \frac{1}{4}\sqrt{3}\cos 2\sigma_k + \frac{3\sqrt{3}}{4}\right],
\end{aligned} \tag{6}$$

where $h = \ell/\sqrt{3}$ for the ET configuration and $h = \ell/\sqrt{2}$ for the IRT. It can be shown [6] that, due to the small eccentricity and inclination of the orbits, the solution given by the above zeroth- and first-order terms differs from the exact Keplerian solution by less than 0.03% making the method of analytical series expansion a useful basis for an analytical model of the motions of LISA/NGO.

Choosing $\delta_1 = 5/8$, the first-order (Keplerian) flexing is minimized in both ET and IRT configurations, giving, with arm lengths of order 1 Gm, an extra angle of respectively $7'$ and $4'$. In table 1, we report some orbit indicators (flexing, breathing angles and Doppler shifts) relative to both IRT and ET configurations for $\delta_1 = 0$ and $\delta_1 = 5/8$. The indicators Δ^+ and Δ^- represent the difference between the maximum and minimum (respectively) value and the *nominal* value of a given parameter, over the six years of the mission.

Table 1. Change of the relevant orbit indicators (arm length, breathing, Doppler modulation) for the three S/Cs, for both IRT and ET configurations, in the standard $\delta_1 = 0$ and modified $\delta_1 = 5/8$ inclination. For each indicator, nominal value, average and deviations Δ^+ and Δ^- (see section 2.2), relative to the nominal value over a mission lifetime of 6 years are shown.

	IRT				ET			
$\delta_1 = 0$	Nominal	Mean	Δ^+	Δ^-	Nominal	Mean	Δ^+	Δ^-
L_{12} (km)	10^6	1001 333	+5210	−969	10^6	1001 088	+3852	−757
L_{23} (km)	10^6	1001 333	+5210	−969	10^6	1001 088	+3859	−752
L_{31} (km)	$\sqrt{2}\,10^6$	1416 098	+4988	−1248	10^6	1001 088	+3852	−757
θ_1 (deg)	45				60	60.00	+0.27	−0.18
θ_2 (deg)	90	90.00	+0.36	−0.26	60	60.00	+0.27	−0.18
θ_3 (deg)	45				60	60.00	+0.27	−0.18
$\Delta\mathbf{v}_{12}$ (m s^{-1})	–	−0.11	+5.00	−5.16	–	0.00	+0.87	−0.87
$\Delta\mathbf{v}_{23}$ (m s^{-1})	–	+0.16	+5.00	−4.55	–	0.00	+0.87	−0.87
$\Delta\mathbf{v}_{31}$ (m s^{-1})					–	0.00	+0.87	−0.87
$\delta_1 = 5/8$	Nominal	Mean	Δ^+	Δ^-	Nominal	Mean	Δ^+	Δ^-
L_{12} (km)	10^6	999 115	+786	−2554	10^6	999 277	+241	−1686
L_{23} (km)	10^6	999 115	+786	−2554	10^6	999 277	+241	−1686
L_{31} (km)	$\sqrt{2}\,10^6$	1412 962	−1251	−1253	10^6	999 277	+241	−1686
θ_1 (deg)	45				60	60.00	+0.09	−0.09
θ_2 (deg)	90	90.00	+0.12	−0.12	60	60.00	+0.09	−0.09
θ_3 (deg)	45				60	60.00	+0.09	−0.09
$\Delta\mathbf{v}_{12}$ (m s^{-1})	–	0.00	+0.27	−0.27	–	0.00	+0.16	−0.16
$\Delta\mathbf{v}_{23}$ (m s^{-1})	–	0.00	+0.27	−0.27	–	0.00	+0.16	−0.16
$\Delta\mathbf{v}_{31}$ (m s^{-1})					–	0.00	+0.16	−0.16

3. The Earth effect

We now include the perturbation due to the Earth.

In the analytic approach, the Earth is assumed at rest in the Hill frame. As shown in [9], in the *rotating frame*, the global dynamics in the coupled fields of Sun and Earth is characterized by secular terms producing, in the long run, a drift *away* from the Earth; this is linear in time in the radial direction and quadratic in the tangential direction.

In order to minimize this quadratic y drift, an intuitive strategy is to choose initial conditions such that LISA/NGO is a little further out at start, approaches the Earth, reaches its minimum distance at mid-mission and departs after that [10]. However, other strategies can be devised that provide better performance of the constellation. An appreciable reduction of the flexing due to the Earth tidal field is in any case possible, over a limited time span, by suitable tuning of all orbital parameters [11–13]. In our analytical approach, in order to keep things simple, we still use three identical orbits (apart for relative phase shifts, see (4)) for the three S/Cs of the constellation and, in addition to the above specs, we try and vary the tilt angle δ_1 and a subset of the initial conditions. We first consider a simplified model, where the Earth describes a circular orbit of radius $R_0 = 1$ AU around the Sun on the xy plane [14, 9]. Introducing the minimum trailing angle TA_0, taking place at time t_0, the Earth coordinates $(x_\oplus, y_\oplus, z_\oplus)$ in the HCW frame are

$$x_\oplus = -R_0(1 - \cos(\mathrm{TA}_0)), \qquad y_\oplus = R_0 \sin(\mathrm{TA}_0), \qquad z_\oplus = 0.$$

We consider its effect as a *constant* + *linear* force to be added to the equations of motion. We define the distance of the Earth from the origin, $d_\oplus = \sqrt{x_\oplus^2 + y_\oplus^2}$, and introduce the perturbation parameter

$$\varepsilon_\oplus = \frac{M_\oplus}{M_\odot}\left(\frac{R_0}{d_\oplus}\right)^3, \qquad \frac{M_\oplus}{M_\odot} = \frac{1}{328\,900} \tag{7}$$

so that the effect of the Earth is given by the perturbation

$$\begin{aligned} f_{\oplus x} &= \varepsilon_\oplus \omega^2 (x_\oplus + C_{11}x + C_{12}y),\\ f_{\oplus y} &= \varepsilon_\oplus \omega^2 (y_\oplus + C_{12}x + C_{22}y),\\ f_{\oplus z} &= \varepsilon_\oplus \omega^2 (z_\oplus - z), \end{aligned}$$

where

$$C_{11} = \frac{2x_\oplus^2 - y_\oplus^2}{d_\oplus^2}, \qquad C_{12} = \frac{3x_\oplus y_\oplus}{d_\oplus^2}, \qquad C_{22} = \frac{2y_\oplus^2 - x_\oplus^2}{d_\oplus^2}. \tag{8}$$

The equations of motion can be solved with the perturbation method and the solutions, to be added to the zeroth- and first-order solutions, are of the form

$$\begin{aligned} x_k^{(E)}(t) &= (A_{k,x} + B_{k,x}t)\sin\omega t + (C_{k,x} + D_{k,x}t)\cos\omega t + E_{k,x} + F_x t,\\ y_k^{(E)}(t) &= (A_{k,y} + B_{k,y}t)\sin\omega t + (C_{k,y} + D_{k,y}t)\cos\omega t + E_{k,y} + F_{k,y}t + G_y t^2,\\ z_k^{(E)}(t) &= (A_{k,z} + B_{k,z}t)\sin\omega t + (C_{k,z} + D_{k,z}t)\cos\omega t. \end{aligned} \tag{9}$$

The integration constants $A_i \ldots G_y$ are defined by the choice of initial conditions (see appendix A). The secular terms appearing in the solution generate the parabolic drift around the RV (see appendix B).

By collecting terms, the orbit of the S/C$_k$ is

$$\mathbf{r}_k(t) = \mathbf{r}_k^{(0)}(t) + \mathbf{r}_k^{(1)}(t) + \mathbf{r}_k^{(E)}(t), \tag{10}$$

where the zeroth- and first-order terms are, respectively, given by (4) and (5) and $\mathbf{r}_k^{(E)}(t)$ is given by (9). The terms growing as t and t^2 in (respectively) $x^{(E)}(t)$ and $y^{(E)}(t)$ vanish when one calculates the relative motion between S/Cs, with F_x and G_y being equal for all S/Cs; therefore, the increase in flexing with time is only due to the secular terms as $t\sin t$ and $t\cos t$.

It is now useful to define some quantities in the heliocentric frame.

- Unit vectors of the rotating frame axes:

$$\begin{aligned} \mathbf{u}_x &= \{\cos(\omega t - \mathrm{TA}_0), \sin(\omega t - \mathrm{TA}_0), 0\},\\ \mathbf{u}_y &= \{-\sin(\omega t - \mathrm{TA}_0), \cos(\omega t - \mathrm{TA}_0), 0\},\\ \mathbf{u}_z &= \{0, 0, 1\}. \end{aligned}$$

- Position of the Earth: $\mathbf{R}_\oplus(t) = R_0\{\cos\omega t, \sin\omega t, 0\}$.
- Orbit of S/C$_k$:

$$\mathbf{R}_k(t) = (R_0 + x_k(t))\mathbf{u}_x + y_k(t)\mathbf{u}_y + z_k(t)\mathbf{u}_z. \tag{11}$$

- LISA/NGO barycenter position: $\mathbf{R}_g(t) = \frac{1}{3}\sum_k \mathbf{R}_k(t)$.
- LISA/NGO arm vectors: $\mathbf{R}_{ij}(t) = \mathbf{r}_{ij}(t) = \mathbf{r}_j(t) - \mathbf{r}_i(t)$.
- LISA/NGO arm lengths: $L_{ij}(t) = |\mathbf{r}_{ij}(t)| = |\mathbf{R}_j(t) - \mathbf{R}_i(t)|$.
- Doppler shifts: $v_{ij}(t) = \frac{\mathrm{d}}{\mathrm{d}t}L_{ij}(t)$.
- Trailing angle:

$$\mathrm{TA}(t) = \frac{180}{\pi}\arccos\left(\frac{\mathbf{R}_\oplus(t)\cdot\mathbf{R}_g(t)}{R_0 R_g(t)}\right).$$

- Breathing angles:

$$\theta_j(t) = \frac{180}{\pi}\arccos\left(\frac{\mathbf{r}_{ij}(t)\cdot\mathbf{r}_{jk}(t)}{L_{ij}(t)L_{jk}(t)}\right).$$

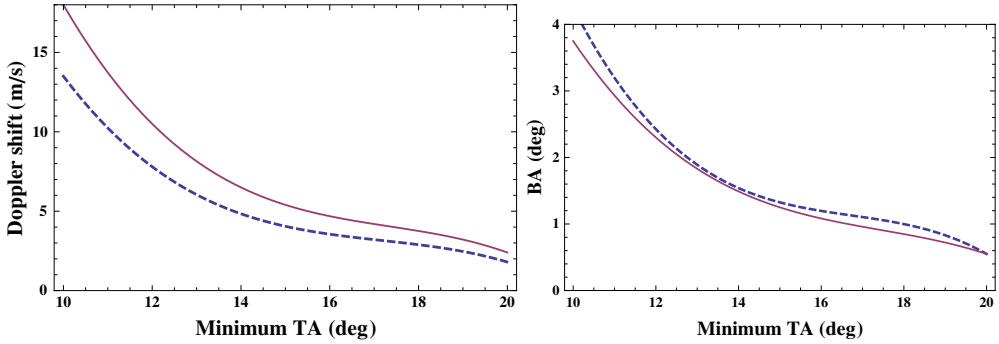

Figure 1. Effect of the Earth (not optimized, analytical derivation). Left: maximum Doppler shift in m s^{-1}. Right: maximum change of the angle between L_{12} and L_{13} (short arms in the IRT). Full curves: ET, dashed curves: IRT. All curves represent the pessimistic scenario, i.e. refer to the one arm that performs worst. No relevant variation appears, however, from one arm to another.

4. Minimization of the flexing

We shall address the choice of an orbit that minimizes the flexing of the arms in three steps: first, by optimizing with respect to the tilt angle only. Then, by perturbing the initial conditions of the three S/Cs in a still analytic approach. Finally, with a fully numerical integration of the S/C orbits, taking into account all major perturbing effects. The mission begins at the time $t_{\rm ini}$ and is assumed to last $\Delta t = 6$ years. We refer to 'mid-mission' or $t_{\rm mid} = t_{\rm ini} + 3$ years as the time half-way into the mission.

In the panels of figure 1, we consider both the ET (full curves) and the IRT (dashed curves) configurations: for these plots the optimization is carried out simply by evaluating the optimal tilt angle over the mission lifetime of six years. Optimization is performed by minimizing the RMS flexing of the three arms over the entire mission duration. The time of closest approach to the Earth is three years after the mission starts and this identifies TA_0.

The requirement on the Doppler shift ($V < 20$ m s^{-1}) shows that we can reduce the minimum TA to less than 10° for both cases (8° for the IRT). By choosing an optimal tilt angle, we can strongly reduce the rms flexing of the arms; this angle always turns out to slightly differ from the canonical 60°. On the other hand, the breathing angle requirement of $\pm 1.5^\circ$ sets a limit at $\mathrm{TA} \simeq 14^\circ$. Breathing appears, therefore, the major obstacle to an appreciable reduction of TA. In the following subsection, we attempt a more general optimization strategy.

4.1. Cost function

In order to extend the optimization to a wider set of parameters, we need to introduce a 'cost function', i.e. a suitable function of the relevant quantities (the flexing) that has to be minimized. To this purpose, we define the following cost function, suitable for both configurations (and therefore different from those proposed in [11]):

$$\sigma^2 = \langle (L_{12} - \langle L_{12} \rangle)^2 + (L_{23} - \langle L_{23} \rangle)^2 + (L_{31} - \langle L_{31} \rangle)^2 \rangle, \tag{12}$$

where

$$\langle \cdots \rangle = \frac{1}{\Delta t} \int_{t_{\rm ini}}^{t_{\rm fin}} \cdots \mathrm{d}t$$

indicates average over the mission time. Although in the IRT case the third arm is not monitored and its flexing could appear as a useless burden to the cost function, we maintained the same σ^2, as defined in (12), for both configurations: minimizing the flexing of all arms is a way to render the triangle 'more rigid' and is an effective strategy, as we shall show, to minimize the breathing angle as well.

4.2. Perturbation of initial conditions—semi-analytic approach

As we extend our optimization strategy, remaining as close as possible to an analytic approach, we must restrict the space of free parameters. Our choice is a subset of the initial conditions of the unperturbed orbits. The Earth produces linear and secular terms in the orbits, as shown by (9). On the other hand, (2) shows that, in general, a linear drift exists in the y component (that we canceled by setting $2\omega x_0 + \dot{y}_0 = 0$). We can, therefore, modify the initial conditions (3) by adding a suitable offset such that these two linear drifts compensate each other.

Therefore, if we set

$$x_{0,k} = -\frac{\dot{y}_{0,k}}{2\,\omega} + \epsilon_k, \quad k = 1, 2, 3, \tag{13}$$

the first two components of the position vector (4) become

$$\begin{aligned} x_k^{(0)} &= \frac{\ell}{2\sin(\pi/n)}\frac{1}{2}\cos\sigma_k + \epsilon_k(4 - 3\cos\omega t), \\ y_k^{(0)} &= \frac{\ell}{2\sin(\pi/n)}\sin\sigma_k - 6\epsilon_k(\omega t - \sin\omega t), \end{aligned} \tag{14}$$

while the third one is unchanged.

In this way trajectories and arm lengths are affected by a perturbation which grows linearly in time. In the expansion (10) we modify only the zeroth-order terms: in principle, the variation should be propagated through the higher order terms, but the contribution is of the order of $\epsilon\ell/R$ in the first-order terms and even smaller in the term describing the Earth effect: we can therefore safely neglect them.

The required amount of this variation can be determined by minimizing the cost function $\sigma^2(\epsilon_1, \epsilon_2, \epsilon_3, \delta_1)$ defined in (12). However, the analytic expression for σ^2 is sufficiently cumbersome to impose a numerical minimization: this, on the other hand, allows us to use the exact equations of motion

$$\begin{aligned} &\ddot{x}_k - 2\omega\dot{y}_k - \omega^2(x_k + R_0) = f_{x,k} \\ &\ddot{y}_k + 2\omega\dot{x}_k - \omega^2 y_k = f_{y,k} \\ &\ddot{z}_k = f_{z,k,} \end{aligned} \tag{15}$$

where $\mathbf{f}_k$ is the Sun+Earth force per unit mass acting on the kth S/C, expressed in the HCW coordinate system.

Setting the RV at $t_0 = t_{\rm mid}$, for the IRT and ET configurations respectively, the minima correspond to

$$\begin{aligned} &\text{IRT}: \ \delta_1 = 0.808, \quad \epsilon_1 = 867\ \text{km}, \quad \epsilon_2 = 519\ \text{km}, \quad \epsilon_3 = 66\ \text{km}, \\ &\text{ET}: \ \delta_1 = 0.894, \quad \epsilon_1 = 523\ \text{km}, \quad \epsilon_2 = 64\ \text{km}, \quad \epsilon_3 = 7\ \text{km}. \end{aligned} \tag{16}$$

The results of the optimization are reported in table 2. The trailing angles in both cases at $t_{\rm ini}$ and $t_{\rm fin}$ are 12.8° (33 Gm from the Earth). The improvement in the values of the performance indicators in the optimized cases is quite evident.

Table 2. Variation of the same orbital indicators as in table 1 (arm length, breathing, Doppler modulation) including the Earth effect (assumed on a circular orbit) corresponding to the optimal data of (16) for the IRT and ET constellations (left and right, respectively).

	IRT				ET			
Not opt.	Nominal	Mean	Δ^+	Δ^-	Nominal	Mean	Δ^+	Δ^-
L_{12} (km)	10^6	1004 681	+47 356	−32 740	10^6	1005 887	+54 846	−36 195
L_{23} (km)	10^6	1005 025	+55 742	−42 716	10^6	1001 830	+16 574	−16 501
L_{31} (km)	$\sqrt{2}\,10^6$	1425 000	+92 213	−59 335	10^6	1006 176	+59 722	−40 762
θ_1 (deg)					60	59.73	+2.71	−3.50
θ_2 (deg)	90	90.30	+4.27	−2.89	60	60.14	+3.91	−3.48
θ_3 (deg)					60	60.11	+4.00	−3.48
$\Delta\mathbf{v}_{12}$ (m s^{-1})	–	−0.36	+8.76	−12.15		−0.30	+10.93	−13.95
$\Delta\mathbf{v}_{23}$ (m s^{-1})	–	+0.49	+13.07	−10.17		+0.06	+5.62	−5.04
$\Delta\mathbf{v}_{31}$ (m s^{-1})						+0.43	+14.72	−12.79
Optimized	Nominal	Mean	Δ^+	Δ^-	Nominal	Mean	Δ^+	Δ^-
L_{12} (km)	10^6	999 363	+14 322	−16 976	10^6	999 440	+13 569	−16 262
L_{23} (km)	10^6	999 284	+14 665	−15 256	10^6	999 228	+12 924	−15 261
L_{31} (km)	$\sqrt{2}\,10^6$	1413 390	+18 695	−21 444	10^6	999 353	+12 793	−15 472
θ_1 (deg)					60	59.99	+1.15	−1.16
θ_2 (deg)	90	90.01	+1.48	−1.50	60	60.00	+1.19	−1.24
θ_3 (deg)					60	60.01	+1.27	−1.26
$\Delta\mathbf{v}_{12}$ (m s^{-1})	–	−0.11	+5.00	−5.16	–	−0.08	+4.88	−5.14
$\Delta\mathbf{v}_{23}$ (m s^{-1})	–	+0.16	+5.00	−4.55	–	+0.01	+5.02	−5.05
$\Delta\mathbf{v}_{31}$ (m s^{-1})					–	+0.14	+4.97	−4.69

4.3. Numerical optimization

In this section, we describe the fully numeric evaluation and minimization of the cost function (12) by solving the exact equations of motion and taking into account the perturbing effect of the Sun, Venus, Earth, Moon, Mars and Jupiter. Their real trajectories $\mathcal{R}_\odot(t), \mathcal{R}_\oplus(t), \mathcal{R}_☽(t), \mathcal{R}_♀(t), \mathcal{R}_♂(t), \mathcal{R}_♃(t)$ in the solar system barycenter (SSB), are provided by the JPL HORIZON ephemerides [15], with the following characteristics:

- Reference epoch: J2000.0.
- XY-plane: plane of the Earth's orbit at the reference epoch.
- X-axis: out along ascending node of instantaneous plane of the Earth's orbit and the Earth's mean equator at the reference epoch.
- Z-axis: perpendicular to the XY-plane in the directional (+ or −) sense of Earth's north pole at the reference epoch.
- Step: 1 day.

In the simplified model used till here, the Sun is assumed at rest at the center of an inertial frame. However, the true inertial frame is represented by the SSB, where the Sun moves in a non-negligible and complex (not simply periodic) way: in this frame the motion of the Earth is substantially different from an ellipse, and therefore the initial condition that we adopted for the S/Cs using (2) is no longer suitable. Moreover, the motion of the Sun is also a relevant source of perturbation. Therefore, to account for these additional effects while maintaining the convenient, Sun-centered HCW description, we must complete the equations of motion with an apparent force deriving from the acceleration of the Sun relative to the SSB.

The equations of motion are as (15), with the forcing term modified as follows:

$$f_{x,k} = (\mathbf{f}_k - \ddot{\mathcal{R}}_\odot)\cdot\mathbf{u}_x, \quad f_{y,k} = (\mathbf{f}_k - \ddot{\mathcal{R}}_\odot)\cdot\mathbf{u}_y, \quad f_{z,k} = (\mathbf{f}_k - \ddot{\mathcal{R}}_\odot)\cdot\mathbf{u}_z,$$

Table 3. Variation of the same orbital indicators as in tables 1 and 2 (arm length, breathing, Doppler modulation) including the effect of the main bodies of the Solar System for the IRT and ET constellations (left and right, respectively).

	IRT				ET			
RV at $t_{\rm ini}$	Nominal	Mean	Δ^+	Δ^-	Nominal	Mean	Δ^+	Δ^-
L_{12} (km)	10^6	1001 798	+19 402	−13 718	10^6	1000 466	+15 507	−15 009
L_{23} (km)	10^6	1002 801	+20 096	−11 128	10^6	1001 006	+27 444	−24 115
L_{31} (km)	$\sqrt{2}\,10^6$	1417 361	+17 162	−9388	10^6	1001 529	+14 365	−11 594
θ_1 (deg)					60	59.99	+1.45	−1.48
θ_2 (deg)	90	89.99	+1.48	−1.48	60	60.05	+1.21	−1.42
θ_3 (deg)					60	59.94	+1.47	−1.08
$\Delta\mathbf{v}_{12}$ (m s^{-1})	–	−0.07	+3.35	−5.14	–	−0.05	+3.32	−5.17
$\Delta\mathbf{v}_{23}$ (m s^{-1})	–	+0.01	+3.44	−4.62	–	−0.08	+3.91	−6.15
$\Delta\mathbf{v}_{31}$ (m s^{-1})					–	+0.03	+3.57	−4.46
Distance (Gm)		32.6–54.5				31.4–53.6		
TA (deg)		12.5–21.0				12.1–20.7		
RV at $t_{\rm mid}$	Nominal	Mean	Δ^+	Δ^-	Nominal	Mean	Δ^+	Δ^-
L_{12} (km)	10^6	1002 735	+25 125	−15 193	10^6	1001 438	+16 132	−14 048
L_{23} (km)	10^6	1002 580	+17 867	−13 678	10^6	1001 331	+22 290	−22 441
L_{31} (km)	$\sqrt{2}\,10^6$	1418 240	+15 529	−3942	10^6	1001 359	+14 976	−10 561
θ_1 (deg)					60	59.99	+1.18	−1.12
θ_2 (deg)	90	90.02	+1.49	−1.49	60	60.00	+1.45	−1.45
θ_3 (deg)					60	60.00	+1.46	−1.46
$\Delta\mathbf{v}_{12}$ (m s^{-1})	–	−0.04	+4.44	−5.44	–	−0.02	+3.86	−3.92
$\Delta\mathbf{v}_{23}$ (m s^{-1})	–	+0.06	+4.56	−4.82	–	+0.01	+5.52	−5.55
$\Delta\mathbf{v}_{31}$ (m s^{-1})					–	+0.04	+3.60	−3.62
Distance (Gm)		36.1–48.6				36.1–48.2		
TA (deg)		13.9–18.7				13.8 –18.5		

where $\mathbf{f}_k$ is the total Newtonian force per unit mass on the kth S/C,

$$\mathbf{f}_k = -\sum_{\alpha} \frac{GM_\alpha}{\|\mathcal{R}_\odot - \mathcal{R}_\alpha + \mathbf{R}_k\|^3}(\mathcal{R}_\odot - \mathcal{R}_\alpha + \mathbf{R}_k), \quad \alpha = \odot, ☿, ♁, ☽, ♂, ♃, \tag{17}$$

and $\mathbf{R}_k$ is the position of the kth S/C in the heliocentric frame (given by (11)).

The amplitude of flexing and breathing scales inversely with the LISA/NGO–Earth distance. This can be intuitively explained as follows: a small flexing is obtained if the constellation rapidly moves away from the Earth, its main source of perturbation to a rigid configuration. However, the overall distance in the mission lifetime must be bound within reasonable values dictated by communication requirements.

An analytical study of the evolution of the Earth–LISA/NGO distance is shown in appendix B where it is verified that the LISA/NGO–Earth distance increases as t^2, after (and before) the RV. Moreover, there is an additional sinusoidal modulation at one-year period due to the eccentricity of the Earth's orbit. We prove that the minima of the sinusoid occur at well-defined epochs that depend on the allowed minimum TA, but not on the epoch t_0 of the RV. Therefore, in order to minimize the Earth–LISA/NGO distance, the optimal choice for t_0 is just one of these minima (B.5). This shows, as mentioned in section 3, that other choices of t_0, different from $t_{\rm mid}$, can minimize flexing and breathing.

In the following we shall discuss two cases: $t_0 = t_{\rm ini}$ and $t_0 = t_{\rm mid}$. The value of TA_0 is chosen as the minimum one that allows a breathing angle smaller than 1.5°, as required. For the two configurations and the two kinds of RVs considered, the minima of the cost function are found at the following values of parameters.

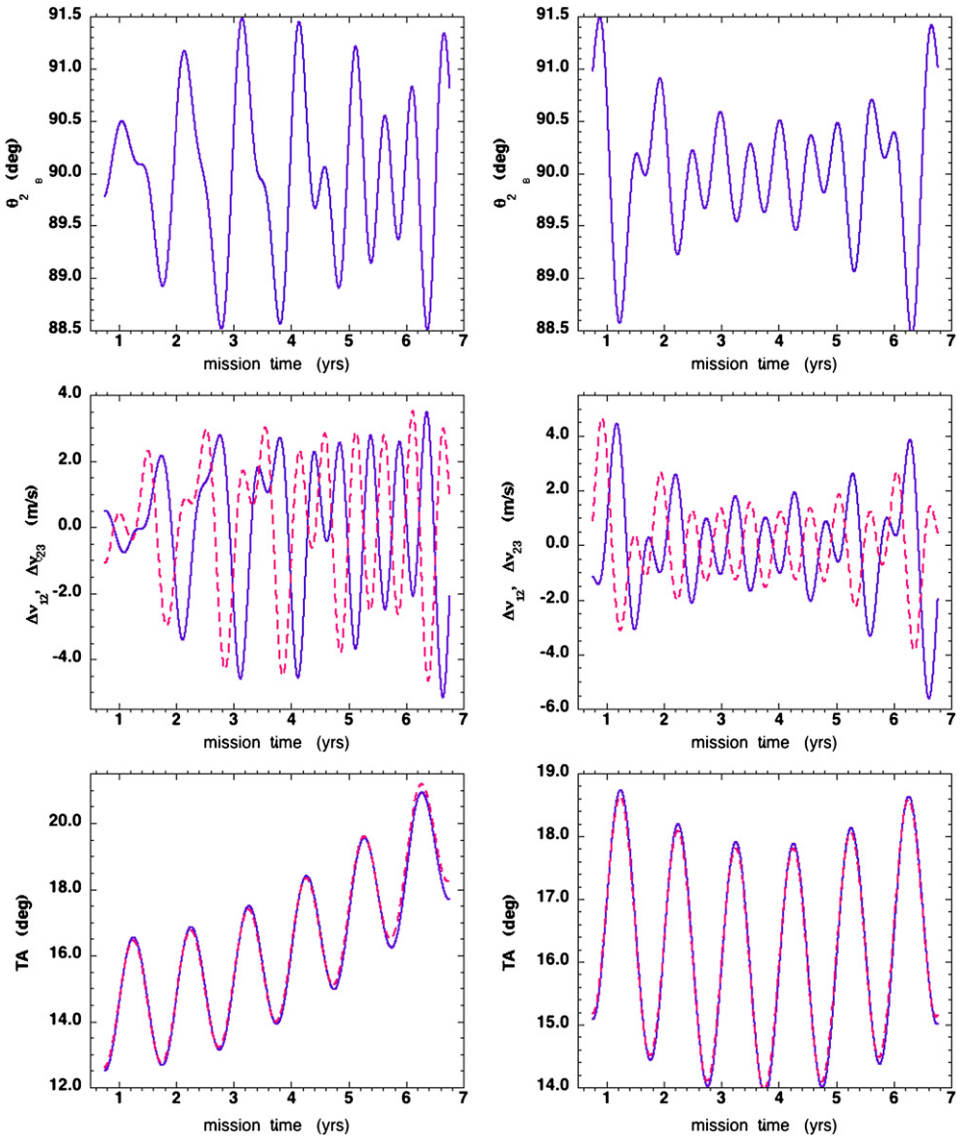

Figure 2. Fully numerical optimization (section 4.3) with respect to both initial conditions and tilt angle for the IRT configuration. Left panels: RV at the beginning of the mission, right panels: RV at mid-mission. Top panels: breathing angles. Center panels: Doppler shifts. Lower panels: distance LISA/NGO–Earth, expressed as TA (red/dashed lines are obtained using (B.6). Ephemerids are taken such that $t = 0$ corresponds to 1 January 2018.

IRT–RV at the beginning ($t_0 = t_{\rm ini}$):

$$\delta_1 = 0.061, \quad \epsilon_1 = 430\ {\rm km}, \quad \epsilon_2 = -113\ {\rm km}, \quad \epsilon_3 = -9\ {\rm km};$$

IRT–RV at mid-mission ($t_0 = t_{\rm mid}$):

$$\delta_1 = -0.290, \quad \epsilon_1 = 28\ {\rm km}, \quad \epsilon_2 = -55\ {\rm km}, \quad \epsilon_3 = -170\ {\rm km};$$

ET–RV at the beginning ($t_0 = t_{\rm ini}$):

$$\delta_1 = 0.473, \quad \epsilon_1 = 70\ {\rm km}, \quad \epsilon_2 = -483\ {\rm km}, \quad \epsilon_3 = 42\ {\rm km};$$

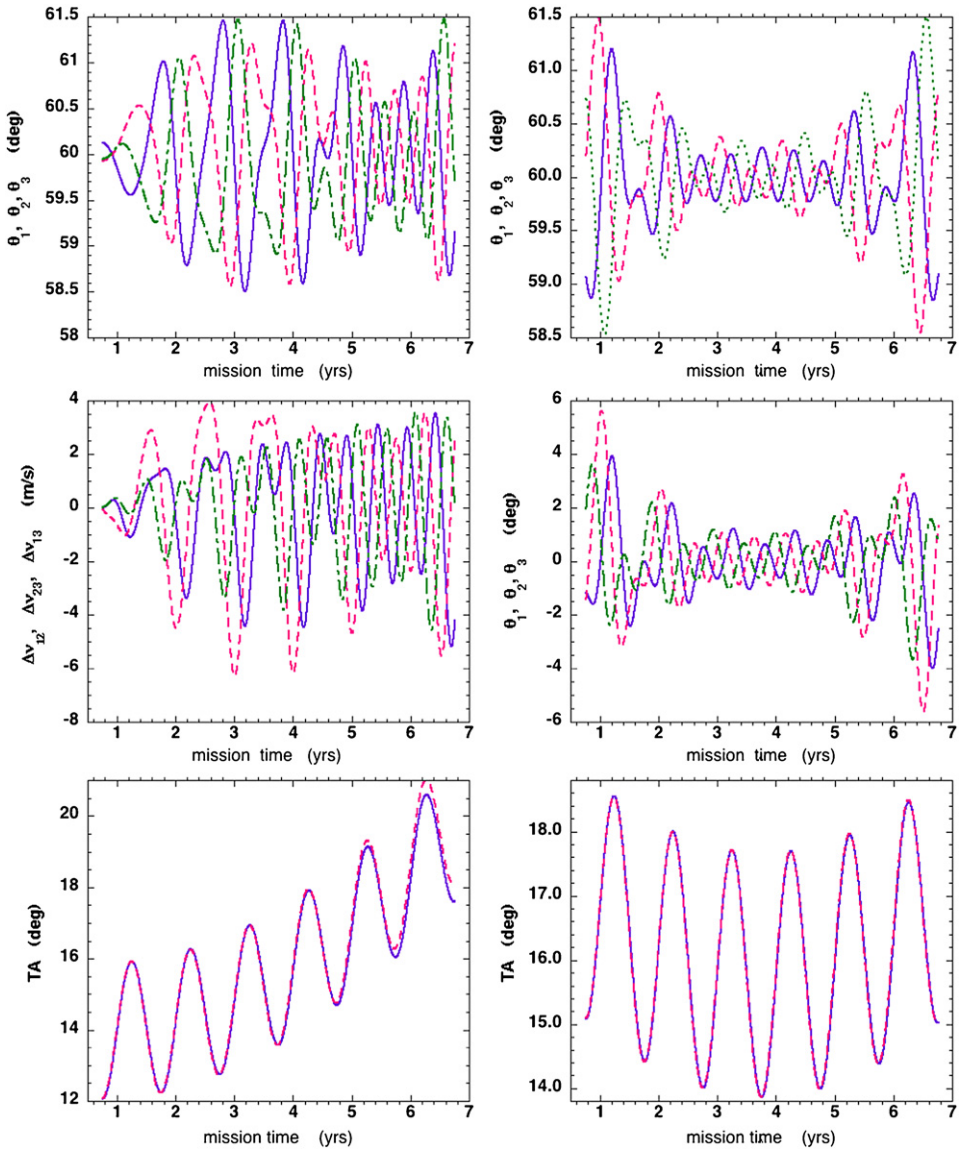

Figure 3. Same as in figure 2, but for the ET configuration. Left panels: RV at the beginning of the mission, right panels: RV at mid-mission. Top panels: breathing angles. Center panels: Doppler shifts. Lower panels: distance LISA/NGO–Earth, expressed as TA (red/dashed lines are analytical predictions obtained using (B.6).

ET–RV at mid-mission ($t_0 = t_{\rm mid}$):

$$\delta_1 = -0.047 \quad \epsilon_1 = 193\ {\rm km}, \quad \epsilon_2 = 52\ {\rm km}, \quad \epsilon_3 = 18\ {\rm km}.$$

Table 3 provides more results and details for the four cases (2 configurations × 2 RV times) considered here.

Some results are also plotted in figures 2 and 3 for IRT and ET configurations, respectively. The ranges of LISA/NGO–Earth distances and trailing angles, as well as the initial conditions for the S/Cs are reported in table 4. We observe that the minimum TA is larger when the RV is

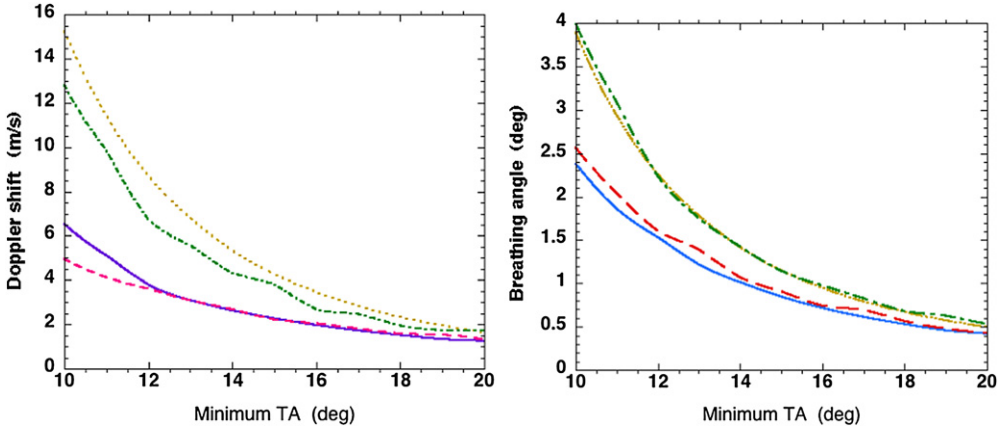

Figure 4. Results of the optimization. Left: maximum Doppler shift in m s^{-1}. Right: maximum change of the angle between L_{12} and L_{13} (short arms in the IRT). Red/dashed curves: ET (RV at the beginning of the mission), blue/full curves: IRT (RV at the beginning of the mission), brown/dotted curves: ET (RV at mid-mission), green/dash-dotted curves: IRT (RV at mid-mission).

Table 4. Initial conditions for the IRT (top) and ET (bottom) configurations in the heliocentric reference frame.

	$X(t_0)$ (Gm)	$Y(t_0)$ (km)	$Z(t_0)$ (km)	$\dot{X}(t_0)$ (km h^{-1})	$\dot{Y}(t_0)$ (km h^{-1})	$\dot{Z}(t_0)$ (km h^{-1})
IRT, RV at t_{ini}			$t_{min} = 5$ Oct. 2018			
S/C1	149 932 288	2412 779	612 461	1721	106 957	0
S/C2	149 588 968	1697 856	2895	1471	107 213	438
S/C3	149 222 635	2401 359	609 567	1729	107 465	0
IRT, RV at t_{mid}			$t_{min} = 7$ Oct. 2018			
S/C1	149 753 118	2 563 623	611 220	1831	107 004	10
S/C2	149 404 775	1 872 191	11 110	1595	107 265	438
S/C3	149 042 293	2 568 312	608 484	1845	107 514	9
ET, RV at t_{ini}			$t_{min} = 5$ Oct. 2018			
S/C1	149 884 804	553 415	500 457	395	107 017	0
S/C2	149 453 230	51 258	248 057	217	107 327	311
S/C3	149 450 059	1052 373	248 057	576	107 326	311
ET, RV at t_{mid}			$t_{min} = 7$ Oct. 2018			
S/C1	149 701 044	1382 500	499 337	987	107 064	9
S/C2	149 267 830	902 343	257 543	824	107 378	307
S/C3	149 266 254	1881 003	237 763	1167	107 370	314

at mid-mission, but the ΔTA is smaller. In general, breathing angles within the specs of 1.5° can be obtained at a smaller distance from the Earth for the ET than the IRT configuration.

Figure 4 shows, in a synoptic way, the results of our optimization procedure with respect to Doppler and breathing angle, versus the minimum trailing angle TA_0. By comparing these optimized results with those derived from the simplest model shown in figure 1, we see that, even considering many more perturbing agents, the optimization manages to reduce both performance indicators by about a factor of 2, at small TA. Again, we see that the requirement on the breathing remains the most stringent constraint. However, while complying with keeping the breathing angle within $\pm 1.5°$, we can address the reduction of flexing following again two opposite strategies: we can set the RV at the beginning of the mission, achieving the lowest

values of TA_0 (we have 12.5° for the IRT and 12.1° for the ET), and accept a maximum ΔTA of about 8.5° in both cases. Else, if RV takes place at mid-mission, we must accept larger values of TA_0 (13.9° for the IRT and 13.8° for the ET), but TA will change much less during the mission: ΔTA is less than 4.8° in both cases.

5. Conclusions

We have shown that the choice of heliocentric orbits for LISA/NGO is a viable solution even when reducing the arm length: this allows a substantial reduction in the TA (with beneficial savings for placement in orbit and communications with the Earth) of an amount that depends on the assumed mission duration. For an expected mission time of six years, the minimum value of the TA can be reduced to about 12°. If a two-link interferometer were preferred for a new, cheaper version of the LISA mission, the IRT would be a viable configuration, as stable as the ET in all of the tests we have computed. The amount of flexing that the constellation undergoes during the mission depends strongly on the initial conditions. The reasons for this behavior lie mostly in the time-dependent perturbations due to the eccentricity of the Earth orbit, and to the motion of the Sun with respect to the SSB. A more detailed analysis of these effects is underway.

Appendix A. Initial conditions for the motion in the Earth field

Equation (9) can be recast in the following, equivalent but more explicit form, where the constants C_{ij} of (8) are folded into the solution:

$$x_k^{(2)} = x_\oplus + 2A_k + 2y_\oplus \omega t + B_k \cos\omega t + C_k \sin\omega t + \ell \frac{(C_{11} + 12C_{22})\cos\sigma_k + 2(2C_{12} + (C_{11} + 4C_{22})\omega t)\sin\sigma_k}{8\sqrt{3}},$$

$$y_k^{(2)} = 4y_\oplus - \left(3\frac{A_k}{2} + 2x_\oplus\right)\omega t - \frac{3}{2}y_\oplus(\omega t)^2 + D_k + 2(C_k\cos\omega t - B_k\sin\omega t) - \ell\frac{(3C_{11} + 16C_{22})\sin\sigma_k - 2(2C_{12} + (C_{11} + 4C_{22})\omega t)\cos\sigma_k}{4\sqrt{3}},$$

$$z_k^{(2)} = E_k\cos\sigma_k + F_k\sin\sigma_k - \frac{\ell}{4}\sigma_k\sin\sigma_k,$$

where the σ_k are the time-dependent phases (4).

The 18 constants $A_k, \ldots, F_k$ are determined by the initial conditions, which are chosen assuming $\left(x_k^{(E)},\ y_k^{(E)},\ z_k^{(E)}\right) = (0, 0, 0)$ at $t = 0$.

They are

$$\begin{aligned}
A_k &= -\ell\frac{2C_{22}\cos\sigma_k^0 - C_{12}\sin\sigma_k^0}{\sqrt{3}},\\
B_k &= -x_\oplus - \frac{\sqrt{3}\ell}{24}\left((C_{11} - 4C_{22})\cos\sigma_k^0 + 4C_{12}\sin\sigma_k^0\right),\\
C_k &= -2y_\oplus + \frac{\sqrt{3}\ell}{24}\left((C_{11} - 4C_{22})\sin\sigma_k^0 - 4C_{12}\cos\sigma_k^0\right),\\
D_k &= \frac{\ell}{2\sqrt{3}}(C_{12}\cos\sigma_k^0 - 2(C_{11} + 3C_{22})\sin\sigma_k^0),\\
E_k &= -\frac{\ell}{4}\sin^2\sigma_k^0, \qquad F_k = -\frac{\ell}{8}\left(2\sigma_k^0 - \sin 2\sigma_k^0\right),
\end{aligned}$$

where $\sigma_k^0 = \frac{2\pi(k-1)}{n}$ are the relative phase shifts of (4) evaluated at $t = 0$.

Appendix B. Distance Earth–LISA/NGO barycenter in epicyclic approximation

Here we calculate the analytic expression for the distance between a particle (i.e. the LISA/NGO barycenter) and the Earth, taking into account the eccentricity of the orbit.

We consider the Earth orbit in the epicyclic approximation (at $t = 0$ in the perihelion) in the inertial frame centered in the Sun:

$$\mathbf{R}_{\oplus}(t) = R_0 \left\{ \cos\omega t + \frac{e}{2}\cos 2\omega t - \frac{3}{2}e, \sin\omega t + \frac{e}{2}\sin 2\omega t, 0 \right\}. \tag{B.1}$$

The LISA/NGO barycenter, as a first approximation, can be considered at rest in the HCW frame at TA_0 degrees from the Earth. In the inertial frame its trajectory is

$$\mathbf{R}_g(t) = R_0\{\cos(\omega t - \mathrm{TA}_0), \sin(\omega t - \mathrm{TA}_0), 0\}.$$

At zero order, the force of the Earth on the particle is

$$\mathbf{f} = \epsilon R_0 \omega^2 \{ f_x + ec_x \cos\omega t + es_x \sin\omega t,\ f_y + ec_y \cos\omega t + es_y \sin\omega t, 0 \}, \tag{B.2}$$

where $e \approx 0.016\,71$ is the eccentricity of the Earth's orbit and

$$\begin{aligned}
&\epsilon = \frac{M_{\oplus}}{4M_{\odot}\sqrt{2 - 2\cos\mathrm{TA}_0}}, \qquad f_x = -2, \qquad f_y = \frac{2}{\tan\mathrm{TA}_0/2},\\
&c_x = \frac{2}{\cos\mathrm{TA}_0 - 1} - 1, \qquad c_y = \frac{1}{\tan\mathrm{TA}_0/2},\\
&s_x = \frac{2}{\tan\mathrm{TA}_0/2}, \qquad s_y = \frac{8}{\cos\mathrm{TA}_0 - 1} + 2.
\end{aligned}$$

The new perturbation parameter ($\epsilon = 2.6 \times 10^{-4}$ for $\mathrm{TA}_0 = 10^{\circ}$) is slightly different from that introduced in (7) to show the explicit dependence on TA_0. The coefficients ec_x, ec_y, es_x and es_y are much smaller than f_x and f_y and, therefore, we neglect the terms proportional to $e\epsilon$ in (B.2) and solve perturbatively the HCW equations, assuming $\mathbf{r}_g = \{0, 0, 0\}$ as the unperturbed motion. We calculate the perturbation $\mathbf{r}_1(t)$ with the assumptions $\mathbf{r}_1(t_0) = \{0, 0, 0\}$ and $\dot{\mathbf{r}}_1(t_0) = \{0, 0, 0\}$, where t_0 is the epoch at which we put the particle at TA_0 degrees from the Earth. Letting $t' = t - t_0$ we have

$$\begin{aligned}
\mathbf{r}_1(t') = \epsilon R_0 \{ & f_x(1 - \cos\omega t') + 2f_y(\omega t' - \sin\omega t'),\\
& 2f_x(\sin\omega t' - \omega t') + f_y(4 - 4\cos\omega t' - 3/2\omega^2 t'^2),\\
& 0\}.
\end{aligned} \tag{B.3}$$

We transform (B.3) in the inertial coordinates using (11) and calculate the distance $d(t)$ of the particle from the Earth using expression (B.1). Finally, we expand in the Taylor series the distance to the first order in e and ϵ:

$$d(t) = d_0 + e\,d_1(t) + \epsilon\,d_2(t) + O(e^2), \tag{B.4}$$

where

$$\begin{aligned}
d_0 &= R_0\sqrt{2 - 2\cos\mathrm{TA}_0},\\
d_1(t) &= \frac{R_0}{\sqrt{2 - 2\cos\mathrm{TA}_0}}[(\cos\mathrm{TA}_0 - 1)\cos\omega t + 2\sin\mathrm{TA}_0 \sin\omega t],\\
d_2(t') &= \frac{R_0}{2\sqrt{2 - 2\cos\mathrm{TA}_0}} f_x\\
&\quad + 2f_y\omega t' - f_x\cos\mathrm{TA}_0 - 2f_y\omega t'\cos\mathrm{TA}_0 + 1/2(-8f_y + 4f_x\omega t'\\
&\quad + 3f_y\omega^2 t'^2)\sin\mathrm{TA}_0 + \cos\omega t'(-f_x + f_x\cos\mathrm{TA}_0 + 4f_y\sin\mathrm{TA}_0)\\
&\quad + (-2f_y + 2f_y\cos\mathrm{TA}_0 - 2f_x\sin\mathrm{TA}_0)\sin\omega t'.
\end{aligned}$$

The term d_0 is a constant and d_1 is a sum of sinusoids with 1 year period. The d_2 term contains linear and quadratic terms in $t - t_0$, and is, therefore, negligible for $t \approx t_0$ because $\epsilon \ll e$ but it becomes dominant for larger t.

The epochs of the relative minima and maxima of $d(t)$ depend on TA_0 but not on t_0. They are found by equating to zero the first derivative of d_1,

$$2\cos\omega t \sin \mathrm{TA}_0 + (1 - \cos \mathrm{TA}_0)\sin\omega t = 0.$$

With the additional condition on the second derivative

$$(1 - \cos \mathrm{TA}_0)\cos\omega t_{\min} - 2\sin \mathrm{TA}_0 \sin\omega t_{\min} > 0,$$

the minima occur at

$$t_{\min,k} = -\frac{1}{\omega}\arctan\left[\frac{2}{\tan(\mathrm{TA}_0/2)}\right] + \frac{2k\pi}{\omega}, \qquad k \in \mathbb{Z}. \tag{B.5}$$

In the same fashion of (B.4), the TA can be obtained, to first order in e, as

$$\mathrm{TA}(t) = \mathrm{TA}_0 + 2e\sin\omega t + \epsilon\left[4f_y(\cos\omega t' - 1) + 2f_x(\omega t' - \sin\omega t') + \tfrac{3}{2}f_y(\omega t')^2\right]. \tag{B.6}$$

Although the epochs $t_{\min}$ are obtained using a first-order approximation, they are in good agreement with the exact values (for an example, see the bottom panels of figuress 2 and 3).

Acknowledgments

We are grateful to Pete Bender, Massimo Cerdonio, Oliver Jennrich, Philippe Jetzer and Bill Weber for useful discussions. We also thank Stefano Vitale for encouragement and support.

References

[1] https://lisa-light.aei.mpg.de/bin/view/Main/WebHome
[2] https://lisa-light.aei.mpg.de/bin/view/ScienceWorkingTeam/YellowBook
[3] Shaddock D *et al* 2006 *AIP Conf. Proc.* **873** 654–60
[4] Bik J J C M, Visser P N A M and Jennrich O 2007 *Adv. Space Res.* **40** 25
[5] Nerem S 2003 http://ccar.colorado.edu/asen5050/lecture12.pdf
[6] Nayak K R, Koshti S, Dhurandhar S V and Vinet J-Y 2006 *Class. Quantum Grav.* **23** 1763
[7] Sweetser T H 2005 Epicycles and oscillations: the dynamics of the LISA orbits *AAS/AIAA Astrodynamics Specialist Conf.* Paper AAS 05-292
[8] Dhurandhar S V, Nayak K R, Koshti S and Vinet J-Y 2005 *Class. Quantum Grav.* **22** 481
[9] Pucacco G, Bassan M and Visco M 2010 *Class. Quantum Grav.* **27** 235001
[10] Dhurandhar S V, Nayak K R and Vinet J-Y 2008 *Class. Quantum Grav.* **25** 245002
[11] Hughes S P 2005 Preliminary optimal orbit design for LISA *25th Annual AAS Guidance and Control Conf.*
[12] Xia Y, Li G Y, Heinzel G, Rüdiger A and Luo Y J 2010 *Sci. China Phys. Mech. Astron.* **53** 179
[13] Li G *et al* 2008 *Int. J. Mod. Phys.* D **17** 1021–42
[14] Cerdonio M, De Marchi F, De Pietri R, Jetzer P, Marzari F, Mazzolo G, Ortolan A and Sereno M 2010 *Class. Quantum Grav.* **27** 165007
[15] http://ssd.jpl.nasa.gov/horizons.cgi